Investigation of CO Binding and Release from Mo-Nitrogenase during Catalytic Turnover†

Linda M. Cameron and Brian J. Hales*

Department of Chemistry, Louisiana State University, Baton Rouge, Louisiana 70803-1804

Received October 27, 1997; Revised Manuscript Received May 6, 1998

ABSTRACT: During enzymatic turnover in the presence of CO, Mo-nitrogenase has been shown to generate two different EPR signals termed lo-CO ($P_{CO} = 0.08$ atm) and hi-CO ($P_{CO} = 0.5$ atm). When the formation of hi-CO is monitored under the conditions of very low electron flux, a 2 min lag is observed prior to the initial detection of the signal followed by a near-linear rate of formation during which the $S = 3/2$ cofactor signal exhibits similar decay kinetics. Increasing the electron flux produces a significant increase in the rate of both the formation of hi-CO and the decay of the $S = 3/2$ cofactor. These results are interpreted in terms of a state of the enzyme (redox or structural) generated only during turnover which is needed to initially bind CO to the cofactor. Under high electron flux conditions, new EPR inflections are observed at $\boldsymbol{g} = 5.78, 5.15$ and $\boldsymbol{g} = 1.95, 1.81$ and tentatively assigned to $S = 3/2$ and 1/2 states of the CO-bound cofactor and 1 equiv of oxidized P cluster, respectively. Sudden removal of CO from the environment results in the slow decay (>10 min) of both the hi-CO signal and CO inhibition of acetylene reduction activity. The use of ethylene glycol to quench enzymatic activity strongly inhibits the decay of hi-CO (in the presence of CO) and the subsequent decay of lo-CO (after removal of CO) but does not prevent the reversible interconversion hi-CO ↔ lo-CO + CO.

The exquisite determination of the structure of the component proteins of Mo-nitrogenase (*1*−*6*) now serves as an invaluable aid to our study of the mechanism of nitrogen fixation. Some of the major questions concerning that mechanism relate to the site(s) of substrate and inhibitor binding as well as the modes of binding and release of these molecules. CO inhibition of nitrogenase has recently been studied to answer some of these questions (*7*−*10*). The results on the kinetics of CO binding and release are presented here.

Carbon monoxide has been shown to be a strong non-competitive inhibitor of all substrate reductions by Mo-nitrogenase, except for dihydrogen evolution (*11, 12*). During CO inhibition, two intense $S = 1/2$ EPR signals are generated (*13*−*16*). One of these signals (lo-CO: 0.08 atm) with $\boldsymbol{g} = [2.09, 1.97, 1.93]$ appears under low pressures while the other (hi-CO: 0.5 atm) with $\boldsymbol{g} = [2.17, 2.06, 2.06]$ occurs at high pressures. Because these signals are only present during enzymatic turnover, they obviously represent mechanistic intermediate states of CO inhibition and, as such, can be used to probe the enzyme during catalysis. Using ^{13}C ENDOR spectroscopy, it has been shown (*7*) that lo-CO corresponds to one CO bound to a metal cluster of the component 1 protein of Mo-nitrogenase from *Azotobacter vinelandii* (Av1) while hi-CO arises from two CO's bound to the same metal cluster. Subsequent ENDOR studies on ^{57}Fe-labeled isotopomers definitively demonstrated that CO binds to the cofactor cluster (i.e., FeMo-co) of Av1 (*8*). Recently, orientation-selective ^{13}C and ^{57}Fe ENDOR spectroscopy has revealed that CO in lo-CO is bound in a bridging fashion while both CO's in hi-CO exhibit terminal binding (*10*). It was also determined (*9*) that the valencies of the metal ions in the resting-state cofactor, lo-CO and hi-CO, are $[Mo^{4+},Fe^{3+},Fe^{2+}_6,S^{2-}_9]^+$. CO binding to nitrogenase also has been investigated with stopped-flow Fourier transform infrared spectroscopy (*17*) which detected a single absorption under low CO concentrations and 3−4 absorptions at high CO concentrations.

The hi-CO and lo-CO signals are now used to monitor their formation and decay during enzymatic turnover and following activity quenching with ethylene glycol. Results from these studies suggest that the formation of these signals requires a redox or structural state of the enzyme that is only induced during catalytic turnover. Once these signals are formed, they can be interconverted in the absence of turnover. Two new EPR signals are detected during high electron flux in the presence of CO and high concentations of ATP. One of these signals arises from singly oxidized P clusters (P^+). The origin of the other signals is not know but is hypothesized to arise from the paramagnetic CO-bound cofactor similar to hi-CO ($S = 1/2$) but in a different spin state ($S = 3/2$).

MATERIALS AND METHODS

Mo-nitrogenase from *Azotobacter vinelandii* was isolated and purified according to published methods (*18*). All procedures were performed anaerobically (O_2 < 1 ppm) in 0.025 M Tris-HCl buffer (pH 7.4) containing 2 mM dithionite ($Na_2S_2O_4$).

Specific activity was monitored by the acetylene reduction assay (10% acetylene in Ar in 13.8 mL rubber-stoppered

† This work was supported by Grant GM 33956 from the National Institutes of Health and by Grant DOA-96-35305-3730 from the Department of Agriculture.

S0006-2960(97)02667-6 CCC: $15.00
Published on Web 06/12/1998

serum vials containing 1.0 mL of MgATP-regenerating solution plus nitrogenase component proteins) using a gas chromatograph (Varian, Model 3700) equipped with a flame ionization detector and fitted with a Porapak T column. The MgATP regeneration solution contained the following: [ATP] = 2.5 mM, 30 mM phosphocreatine, 0.125 mg/mL creatine phosphokinase, [$MgCl_2$] = 5 mM, [$Na_2S_2O_4$] = 20 mM, 38 mM TES−KOH, pH 7.4. For solutions that had a 5× increase in ATP, only the ATP concentration was increased without an increase in any of the other components. Unless otherwise stated, all reactions were conducted at 30 °C in a shaker water bath (100 rpm). Reactions for activity measurements were terminated by the addition of 0.1 mL of TCA (30%). When H_2 evolution was used to monitor activity, a thermal conductivity gas chromatograph was used (Shimadzu, Model GC-8A, fitted with a 0.5 Å 80/100 mesh molecular sieve column). Protein concentrations were determined by the biuret method. Due to the large amount of protein needed for the EPR kinetic profiles (all listed experiments were repeated at least 4 times), several different batches of protein were used. The specific activity range for Av1 was 1700 ± 200 nmol of C_2H_4 produced min^{-1} mg of $protein^{-1}$ and 1600 ± 175 nmol of C_2H_4 produced min^{-1} mg of $protein^{-1}$ for Av2. Metal analysis for Av1 was performed using an ICP emission spectrometer (ARL, Model 3400) as previously described (*19*) and found to be 21 ± 3 Fe atoms per protein and 1.6 ± 0.2 Mo atoms per protein.

In the gas-exchange experiments, turnover reaction vials were prepared as described above for specific activity measurements except that a known quantity of CO (Scott Specialty Gases) was added to the headspace. To exchange this gas, the headspace was pumped off and replaced with Ar or C_2H_2 (10% in Ar) in three evacuation−charge cycles requiring no longer than 2 min. Samples were continually agitated during the procedure to facility gas exchange.

Quenching experiments with ethylene glycol (EG) were performed as follows. Anaerobic buffer (0.025 Tris-HCl, pH 7.4) was diluted with EG (80%) and contained 20 mM dithionite. To quench a turnover reaction, an equal volume of the EG mixture was added to make a final solution of 40% EG. This amount of EG previously had been shown (Blanchard and Hales, unpublished) to stop enzymatic turnover within <1 s. Gas-phase samples were extracted for C_2H_4 or H_2 production determinations, and a liquid sample was anaerobically placed in an EPR tube and rapidly frozen for subsequent spectral analysis.

EPR spectra were recorded at cryogenic temperatures on a Bruker ER 300D spectrometer interfaced to a Bruker 1600 computer for data storage and manipulations. An Oxford Instrument ESR-900 helium flow cryostat positioned in a TE_{102} cavity was used to reach low temperatures. Temperature was monitored and controlled using an Oxford Instrument Model ITC4 temperature controller with a digital readout. Spin concentration determinations were performed on the Bruker computer by double integration of the spectral envelope using Cu(II)EDTA as a spin standard. All spin concentration determinations were performed at ≥10 K to avoid saturation effects often encountered with Cu(II)EDTA at lower temperatures.

Values for *D* (the axial zero-field splitting parameter) were determined by curve-fitting Boltzmann distribution expressions for the relative populations of the doublets in question to Curie law corrected spectral areas recorded in temperature-dependent depopulation experiments. EPR spectral assignments for half-integer spin systems were effected by numerical determination of possible *g*-factors in the weak-field limit using the computer program "RHOMBO" (*20*), which was generously furnished by Professor W. R. Hagen.

RESULTS

Having established that lo-CO and hi-CO originate from one and two CO molecules, respectively, bound to the cofactor, it is now important to determine the mechanism for the formation and decay of these signals. What is known is that these signals are produced only during enzymatic turnover and disappear upon its termination.

Signal Formation: Low Electron Flux. To investigate the mechanism for the production of these signals, their formation was monitored under the conditions of very low electron flux when only H_2 evolution occurs. Low flux was used to decrease the rate of formation to a value that is easily monitored by EPR spectroscopy. Since Av2 is the electron donor to Av1, very low electron flux can be achieved by having a small Av2-to-Av1 concentration ratio. Samples were prepared with [Av2]/[Av1] = [0.4 μM]/[40 μM] = 1:100, a component ratio chosen because it previously had been shown (*21, 22*) that similar protein ratios require 5−10 min to achieve steady-state conditions. In these experiments, the $S = 3/2$ EPR signal of the cofactor (M) was used to monitor the extent of reaction. In the absence of CO, this cofactor signal decreases to 40−50% of its original value (Figure 1A). It is well established (*23*) that the first electron transferred reduces the cofactor (M) to an EPR-silent state (M^-). During very low electron flux, the steady-state reaction mixture consists of about half of the cofactors in the EPR-active $S = 3/2$ M state and half in state M^- (*22*, *24*). The dip in the amplitude of the $S = 3/2$ signal below 50% prior to steady-state conditions (Figure 1A) is not unusual (*25*) and is presumably due to an initial overproduction of M^-. The extent of this initial dip varied among different samples tested and typically ranged from 40% to 20%. When 100% CO is present in the gas phase (Figure 1A), this dip is nearly eliminated while the initial (0−3 min) decay profile is unaffected. The reason CO eliminates this dip is unknown.

The time-dependent formation of hi-CO reveals several important features. First, while there is an immediate detectable decay in the $S = 3/2$ cofactor signal upon initiation of the reaction, a lag (∼2 min) occurs prior to the initial detection of hi-CO (Figure 1B). Second, at no time was any lo-CO detected. Third, after the cofactor signal has reached its pseudo-steady-state concentration in about 10 min, hi-CO continues to increase in concentration with a slow, near-linear rate ($\approx 5 \times 10^{-5}$ s^{-1}) for over 1 h (Figure 1A). During this same time interval, the $S = 3/2$ cofactor signal exhibits a similar slow decay, suggesting the slow conversion of native cofactor to CO-bound cofactor, such that the net reaction is

$$\mathrm{EPM}\ \{S = 3/2\} + 2\mathrm{CO} \xrightarrow{\text{turnover conditions}} \mathrm{EP[M(CO)_2]}\ \{S = 1/2, \text{hi-CO}\} \quad (1)$$

In the above equation, E symbolizes half of the Av1

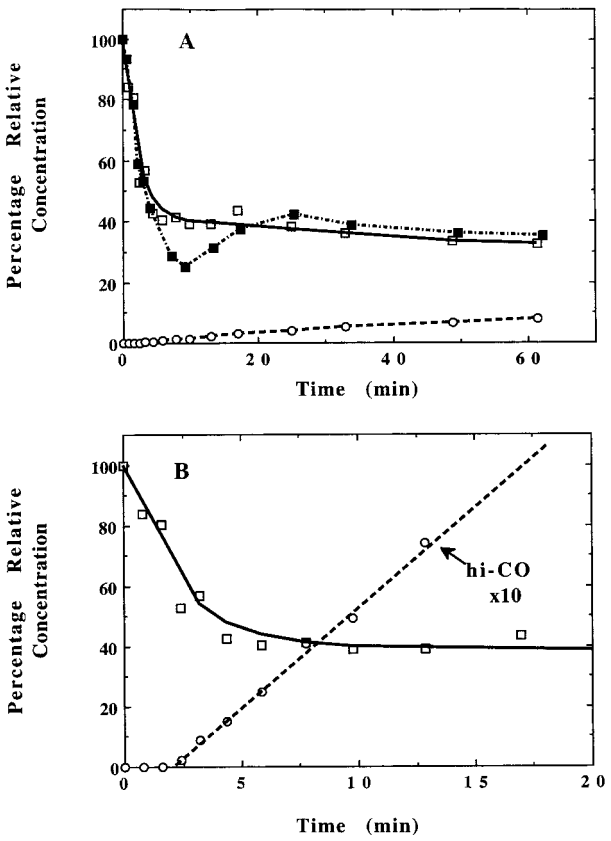

FIGURE 1: (A) Time course of the decrease in amplitude of the $S = 3/2$ cofactor signal (M) during turnover in the absence (■) and presence (□) of 1.0 atm of CO. Also plotted is the intensity (normalized to the concentration of the initial cofactor signal) of hi-CO (○). (B) Expansion of (A) during the early time course showing the lag prior to the initial detection of hi-CO. Experimental conditions: [Av2]/[Av1] = [0.4 μM]/[40 μM] = 1:100; atmosphere either 100% Ar (■) or CO (□, ○).

apoprotein with P and M representing the corresponding P cluster and cofactor in their as-isolated oxidation states (Table 1).

In an attempt to similarly monitor the formation of lo-CO during very low electron flux, the above experiment was repeated using lower CO pressures (P_{CO}) to favor the formation of only lo-CO. However, while decreasing P_{CO} resulted in a decrease in the amount of hi-CO formed, at no P_{CO} tested (1.0 atm $\geq P_{CO} \geq$ 0.001 atm) was any lo-CO ever detected. This is in contrast with results at higher electron flux where decreasing P_{CO} to 0.05 atm results in a shift of the EPR spectrum from hi-CO to lo-CO (*16*). In other words, lo-CO is not detectable under low electron flux conditions and may not be a necessary intermediate state in the production of hi-CO. This is contrary to the results from recent ST-FTIR experiments which suggest the formation of lo-CO prior to hi-CO (*17*). These latter experiments, however, monitor *all* CO-bound forms of the enzyme (both EPR-active and EPR-silent) and were performed at higher electron flux.

Signal Formation: Increasing Flux. The effect of increasing the electron flux (by increasing the component ratio [Av2]/[Av1] from 1:100 to as high as 1:5) was investigated. In the absence of CO, increasing the electron flux results in (1) an increase in the rate of the initial decay of M and (2) a decrease in the final steady-state concentration of M from around 50%, as observed at very low flux (Figure 1), to about 10% at the 1:5 protein ratio (*26*−*29*). This result will be discussed in more detail below.

Similar results are obtained for hi-CO formation when CO is present. Namely, increasing the electron flux results in (1) an increase in the rate of formation of hi-CO (from 5×10^{-5} s^{-1} to as high as 0.25 s^{-1}) and (2) a decrease in the final steady-state concentration of hi-CO. The similarity in the electron flux dependency of the steady-state concentration of M (in the absence of CO) and hi-CO (when CO is present) is consistent with our hypothesis (*9*) that hi-CO represents CO bound to the cofactor with the same oxidation state as M (eq 3 and Table 1).

The highest component ratio used in the above experiments ([Av2]/[Av1] = 1:5) is still well below the saturation limit for Av2 (ratio > 4:1). An EPR investigation of turnover with component ratios greater than 1:5 presents a problem. To detect EPR signals during turnover, a relatively high Av1 concentration is required (≈40 μM). At this enzyme concentration and at component ratios above 1:5, the amount of ATP normally present in the regeneration system quickly becomes limiting. When hi-CO was monitored at the higher 1:1 component ratio using a 5× increase in [ATP], two *new* signals became detectable (Figure 2B), one with inflections at $g = 5.78$ and 5.15 and the second at $g = 1.95$ and 1.81. These signals were not observed under identical conditions when either CO was absent or [ATP] was not increased. All of the remaining experiments described below were performed at a 1:5 [Av2]/[Av1] component ratio and normal [ATP].

Signal Decay during Turnover. The rates of decay of hi-CO and lo-CO during turnover were also investigated. Although both lo-CO and hi-CO are known to disappear upon elimination of CO from the gas phase (i.e., CO binding is reversible), the actual rates of release of CO:

$$\mathrm{EP[M(CO)_2]\ \{hi\text{-}CO\} \leftrightarrow EP[M(CO)]\ \{lo\text{-}CO\} + CO} \quad (2)$$

$$\mathrm{EP[M(CO)]\ \{lo\text{-}CO\} \leftrightarrow EPM\ \{}S = 3/2\} + \mathrm{CO} \quad (3)$$

$$\mathrm{EP[M(CO)_2]\ \{hi\text{-}CO\} \leftrightarrow EPM\ \{}S = 3/2\} + 2\mathrm{CO} \quad (4)$$

have not been measured. To determine these rates, samples ([Av2]/[Av1] = 1:5) were prepared in the presence of 0.1 atm of CO, 0.1 atm of C_2H_2, and 0.8 atm of Ar and allowed to incubate for 5 min at room temperature (about 23 °C) to generate an intense hi-CO signal. These samples were subsequently evacuated and flushed 3 times with 10% C_2H_2 in Ar with agitation, and the time course of the hi-CO and M ($S = 3/2$) signals was monitored by EPR spectroscopy. Over 10 min was required (Figure 3) for the full decay of hi-CO with the simultaneous regeneration of the cofactor $S = 3/2$ signal, suggesting a slow rate of release of CO from the cofactor during turnover. The reason the decay profile in Figure 3 is nonexponential is unknown but suggests that the decay mechanism is not a simple first-order reaction. Similar monitor of the decay of lo-CO showed only low concentrations at early time points, suggesting either that the decay of lo-CO is at least as fast as that of hi-CO [i.e., rate (3) ≥ rate (2)] or that both CO molecules are released from the cofactor at the same time (eq 4 is the dominant reaction).

Table 1: Enzyme States

state	identity of state	P cluster spectrum	cofactor spectrum
known states			
EPM	resting	$S = 0$	$S = 3/2$ $g_{\pm 1/2} = [4.32, 3.68, 2.01]$
EP[M^-]	enzymatically reduced	$S = 0$	$S =$ integer (EPR-silent)
EP[M(CO)]	lo-CO	$S = 0$	$S = 1/2$ $g = [2.09, 1.97, 1.93]$
EP[$M(CO)_2$]	hi-CO	$S = 0$	$S = 1/2$ $g = [2.17, 2.06, 2.06]$
E[P^+]M	chemically oxidized	$S = 1/2$ $g = [2.06, 1.95, 1.82]$ $S = 5/2$ $g_{\pm 1/2} = [6.67, 5.30, (1.97)]$[a]	$S = 3/2$ $g_{\pm 1/2} = [4.32, 3.68, 2.01]$
hypothesized states (this paper)			
E*PM	activated	$S = 0$	$S =$ half-integer
E*P[M^-]	activated, enzymatically reduced	$S = 0$	$S =$ integer (probably EPR silent)
E*P[$M^-(CO)_n$]	ditto with CO bound ($n = 1$ or 2)	$S = 0$	$S =$ integer (probably EPR silent)
E*P[$M(CO)_2$] or [$EP^+M(CO)_2]^{2-}$	activated or doubly reduced with CO bound	$S = 0$	$S = 3/2$ $g_{\pm 1/2} = [2.64, 5.15, (1.75)]$ $g_{\pm 3/2} = [(1.39), (1.12), 5.78]$

[a] *g*-Factors in parentheses predicted but not observed.

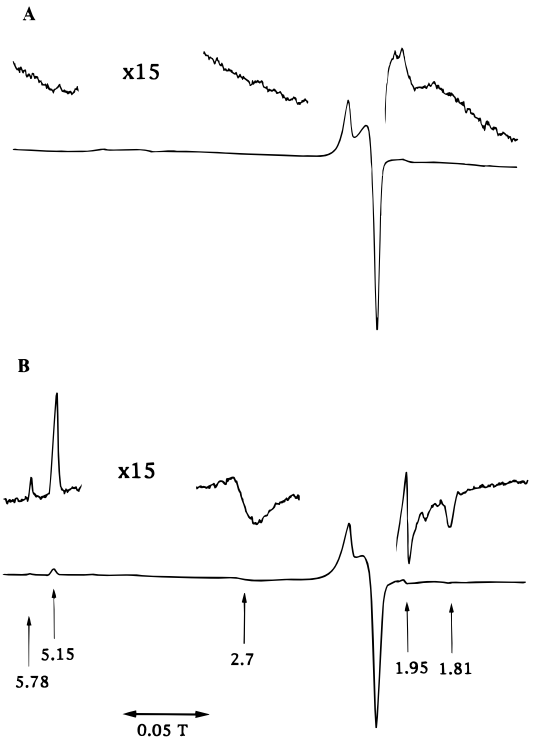

FIGURE 2: Electron flux dependency of the EPR spectrum of hi-CO. Experimental conditions: (A) [Av2]/[Av1] = [8 μM]/[40 μM] = 1:5; [CO] = 1 atm; [ATP] = 12.5 mM (5× normal concentration); [$MgCl_2$] = 25 mM; [$Na_2S_2O_4$] = 20 mM; 50 mM TES−KOH, pH 7.4; following a 10 min incubation at 30 °C, samples were rapidly frozen in liquid N_2; (B) conditions identical to those in (A) except that [Av2]/[Av1] = [40 μM]/[40 μM] = 1:1. Spectrometer parameters: microwave frequency = 9.44 GHz; microwave power = 15 mW; center field = 0.26T; field sweep = 0.32 T; modulation amplitude = 0.5 mT; Temperature = 8 K; inserts in (A) and (B) at gain 15× that used for full spectra.

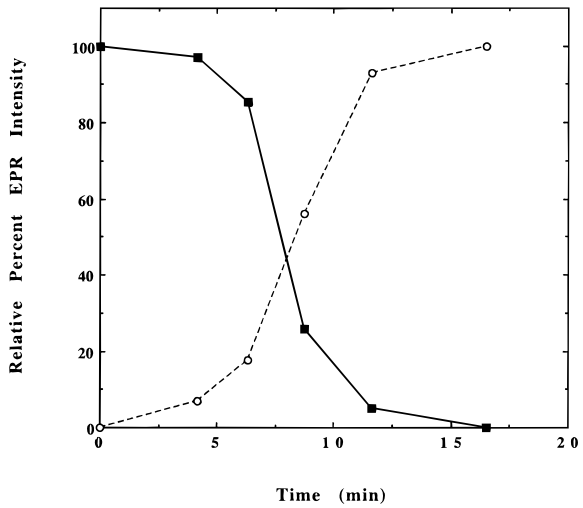

FIGURE 3: Time course of the intensity of hi-CO (■, solid line) and $S = 3/2$ (○, dashed line) cofactor signals during turnover following exchange of the gas phase from CO (10%)/C_2H_2 (10%)/Ar to C_2H_2 (10%)/Ar. Time zero represents point at which gas exchange occurred. Experimental conditions: (A) [Av2]/[Av1] = [4 μM]/[20 μM] = 1:5; [ATP] = 2.5 mM; [$MgCl_2$] = 5 mM; [$Na_2S_2O_4$] = 20 mM; 38 mM TES−KOH, pH 7.4; At set time intervals following gas exchange, samples were extracted from the reaction mixture (incubation at 30 °C), transferred to Ar-filled EPR tubes, and rapidly frozen in liquid N_2.

The slow release of CO implies that there should be a similar slow decay in the inhibitory effects of CO following sudden removal of CO from the atmosphere. To test this, the above experiment was repeated while monitoring C_2H_4 production (Figure 4). Upon evacuation of CO from the gas phase and replacement with 10% C_2H_2 in Ar, inhibition of acetylene reduction activity persisted and required well over 5 min to return to near-linear activity (Figure 4). Therefore, both the time-dependent decay of hi-CO and resumption of normal acetylene reduction activity suggest that the rate of dissociation of CO from the cofactor is slow during turnover.

Signal Decay upon Rapid Termination of Turnover. The above experiments monitored the rate of CO binding and release from nitrogenase *during active catalysis*. It is known that CO does not bind to the cofactor in the resting enzyme; the process requires active turnover. It is possible that turnover similarly influences the ability of CO to be released

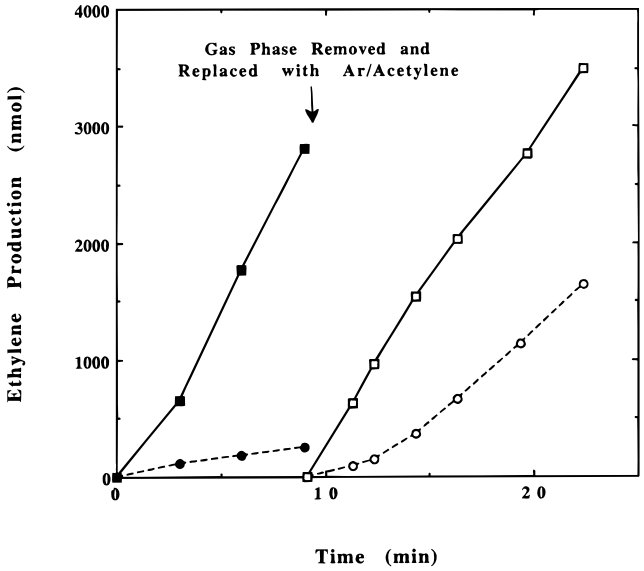

FIGURE 4: Effect of exchange of the gas phase on acetylene reduction activity. Conditions as in Figure 3 except that [Av2]/[Av1] = [4 μM]/[20 μM] = 1:5. Identical samples were prepared; one was incubated in C_2H_2 (10%)/Ar (■, □) while the other initially contained CO (10%)/C_2H_2 (10%)/Ar (●, ○). At 10 min, after initial incubation (■, ●), gas exchange to C_2H_2 (10%)/Ar occurred, and ethylene formation was again monitored (□, ○). The reason full, noninhibitory activity is not obtained with the sample initially exposed to CO (○) is unknown but probably arises from the presence of small residual amounts of CO not removed during the gas exchange cycle.

from the enzyme. It has recently been demonstrated (Blanchard and Hales, unpublished results) that the addition of 40% ethylene glycol (EG) to a turnover sample of nitrogenase rapidly (within <1 s) quenches enzymatic activity and that this quenching is reversible (i.e., full activity is exhibited upon removal of EG). Turnover samples containing 0.1 atm CO were prepared identical to those described above, and their activity was quenched by EG (an equal volume of 80% EG in buffer with 2 mM dithionite was added to the reaction for a final concentration of 40%). Following quenching, the hi-CO signal persisted (Figure 5A) *as long as CO was present in the gas phase*. This result can be contrasted with those obtained (*16*) during slow termination of turnover (caused by the gradual depletion of limiting ATP) in which the hi-CO signal *disappeared*. The rapid quenching with ethylene glycol appears to have "frozen in" or stabilized the hi-CO signal.

When CO was removed from the gas phase of the EG-quenched samples, hi-CO converted into lo-CO (Figure 5B). The further decay of lo-CO into M required over an hour (Figure 5C); EG quenching appears to greatly inhibit the release of the single bound CO molecule of lo-CO even in the absence of CO in the gas phase. Surprisingly, when CO was added back to these samples, lo-CO converted back into hi-CO even though the enzyme was no longer undergoing turnover (Figure 5D). Similar addition of CO to EG-quenched samples initially prepared in the *absence* of CO (so that neither lo-CO nor hi-CO is generated) did not result in the generation of either lo-CO or hi-CO. The generation of lo-CO and hi-CO requires the presence of active turnover, but the interconversion between them does not.

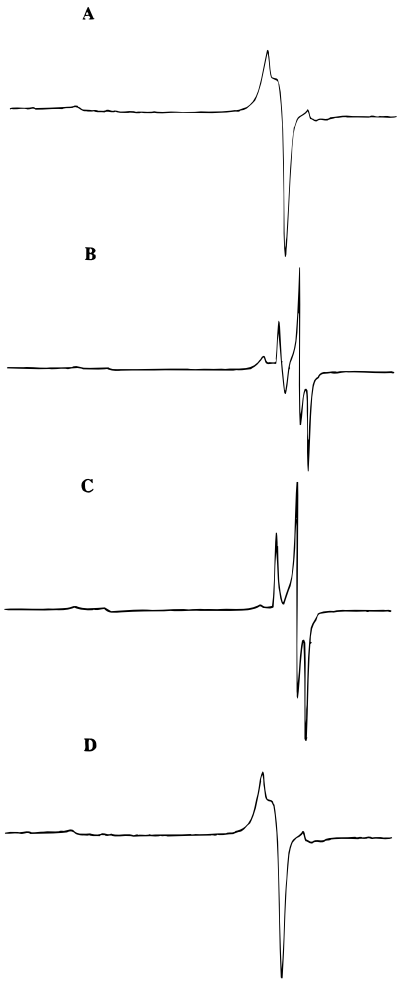

FIGURE 5: Effect of ethylene glycol (EG at 40%) quenching on EPR spectra of hi-CO and lo-CO. Experimental and spectrometer conditions the same as those in Figure 2A. (A) Spectrum recorded 5 min after EG quenching (sample is still in the presence of 1.0 atm of CO). (B) Spectrum recorded 10 min after gas exchange (CO to Ar) of (A). (C) Same as (B) except 20 min after exchange (i.e., 30 min after EG quenching) of (A). (D) Spectrum of (C) following gas exchange (Ar back to CO) and recorded 5 min later. Small low-field inflections in all of the above spectra correspond to the g = 4.3, 3.6 signals of residual cofactor (M) without bound CO.

DISCUSSION

In the discussion below, the terms 'hi-CO' and 'lo-CO' will be used to refer to the two different CO-induced S = 1/2 EPR *signals* while the term 'hi-CO structure' will be used to describe the protein with 2 CO molecules bound to the cofactor. During turnover, the hi-CO structure probably exists as a dynamic mixture of different structural and/or redox states, where at least one of these states is EPR-active and exhibits the hi-CO signal. The same is true for the lo-CO structure. It is important to remember that in the experiments described above *only the EPR-active form is being monitored* (i.e., only a fraction of all of the different enzyme forms).

Which oxidation state of the cofactor is associated with hi-CO and lo-CO can be deduced (*9*). The protein-bound cofactor and the extracted cofactor have been studied extensively using spectroscopic (*23*, *30*−*32*), chemical (*30*, *33*), and electrochemical (*34*) techniques which show the existence of three oxidation states, M^+, M, and M^-, where

only states M and M^- have been detected during turnover (*23*). We previously suggested (*9*) that the same three oxidation levels exist for the CO-bound cofactor. If this is true and since the M state is the only half-integer spin state of the three, the $S = 1/2$ lo-CO and hi-CO signals correspond to CO bound to this oxidation state. The quenching studies described in this paper also support this suggestion. The facts that EG quenched hi-CO and lo-CO can be interconverted in the *absence* of turnover by simply changing the atmospheric CO concentration and that extensive pumping on quenched lo-CO slowly converts it into M suggest that lo-CO, hi-CO, and M all correspond to the same oxidation state of the cofactor (Table 1). The valence assignment of this state was recently determined (*9*) to be $[Mo^{4+}, Fe^{3+},Fe^{2+}_6,S^{2-}_9]^+$.

Formation of Hi-CO. The formation of the hi-CO structure must require a state (X) that is generated during turnover:

$$\mathrm{EPM} + 2\mathrm{CO} \xrightarrow{\text{turnover conditions}} \mathrm{X} + 2\mathrm{CO} \rightarrow \text{hi-CO structure} \quad (5)$$

Although state $EP[M^-]$ is generated during turnover, its steady-state concentration is not dramatically affected by changes in electron flux and possibly varies between 30% and 80%. In other words, if the hi-CO structure is formed by CO reacting with $EP[M^-]$ (i.e., $X = EP[M^-]$), its rate of formation similarly would not be expected to increase greatly with electron flux. This is not what is observed. The rate of formation of hi-CO increases by several orders of magnitude (in our experiments an increase was observed from 5×10^{-5} to 0.25 s^{-1}) with increasing electron flux. Therefore, X most likely represents a state (reduction and/or structural) different from either EPM or $EP[M^-]$ whose steady-state concentration increases greatly with electron flux.

Reduction State. The most popular kinetic model for nitrogen fixation involving different redox states of the enzyme is that developed by Thorneley and Lowe (*35*−*38*). Using the notation introduced above, a simplified representation of the Thorneley−Lowe (TL) reaction mechanism (*22*) during low flux is

$$\underset{S=3/2}{\mathrm{EPM}} + e^- \rightarrow \underset{\text{EPR-silent}}{\mathrm{EP[M^-]}} \quad (6)$$

$$\mathrm{EP[M^-]} + e^- \rightarrow [\mathrm{EPM}]^{2-} \quad (7)$$

$$[\mathrm{EPM}]^{2-} + 2\mathrm{H^+} \rightarrow \mathrm{EPM} + \mathrm{H_2} \quad (8)$$

In these reactions, e^- symbolizes the electrons transferred to the cofactor from reduced Av2 (for simplicity, Av2 oxidation and MgATP hydrolysis have not been included). The TL mechanism predicts that $EP[M^-]$ can be reduced to $[EPM]^{2-}$ which can either undergo further reduction (only significant during high electron flux) or evolve H_2 (eq 8) and relax back to [EPM] (dominant during low flux). The notation $[EPM]^{2-}$ is used to symbolize the doubly reduced state since the actual sites of the two electrons (i.e., cofactor, P-cluster, or protein) are unknown. [In the notation commonly used in the TL model, state $[EPM]^{2-}$ is represented as E_2H_2 while EPM and $EP[M^-]$ are analogous to E_0 and E_1H, respectively (*35*−*38*)].

During low flux, EMP and $EP[M^-]$ are the dominant states of the enzyme with only a small steady-state concentration of $[EPM]^{2-}$ present [rate (8) > rate (7) = rate (6)]. Therefore, CO could bind to $[EPM]^{2-}$ to form the hi-CO structure:

$$[\mathrm{EPM}]^{2-} + 2\mathrm{CO} \rightarrow \mathrm{EP[M(CO)_2]}^{2-} \quad (9)$$

$$\mathrm{EP[M(CO)_2]}^{2-} + 2\mathrm{H^+} \rightarrow \mathrm{EP[M(CO)_2]} + \mathrm{H_2} \quad (10)$$

If rate (8) ≫ rate (9), then during low electron flux most of $[EPM]^{2-}$ would evolve H_2 evolution with only a small amount being converted into the hi-CO structure (eq 9 and Figure 1). Increasing the electron flux would directly increase the rate at which $[EPM]^{2-}$ is re-formed, resulting in an increase in the observed rate of formation of hi-CO.

Structural State. X could also be a structural state of the enzyme different from the resting state. One possibility is that every electron transfer from the Fe protein to the MoFe protein (with ATP hydrolysis) might activate E to a "ready" or "open" structure E*. For example, during the first electron transfer

$$\mathrm{EPM} + e^- \rightarrow \mathrm{E^*P[M^-]} \quad (11)$$

A similar structural change has previously been proposed (*39*). The conversion of E into E* would occur during every electron transfer. If left on its own, this structure would relax to its original "resting" or "closed" structure without a change in the redox state of the enzyme:

$$\mathrm{E^*P[M^-]} \rightarrow \mathrm{EP[M^-]} \quad (12)$$

In this hypothesis, structure E* is required before CO can bind to the cofactor:

$$\mathrm{E^*P[M^z]} + n\mathrm{CO} \rightarrow \mathrm{E^*P[M^z(CO)_n]} \qquad n = 1 \text{ or } 2 \quad (13)$$

(Note that the ability of $E^*P[M^z]$ to bind CO need not be dependent on the redox state z of the enzyme.) If during very low electron flux the rate of relaxation is faster than the rate of electron transfer, the steady-state concentration of E* will be small, resulting in a slow rate of formation of the hi-CO complex (Figure 1). As the electron flux increases, this situation reverses, and the enzyme will remain in state E*, resulting in an increase in the steady-state concentration of E* and an increase in the observed rate of formation of the hi-CO structure.

This structural interpretation of CO binding should also be valid for substrate binding. The X-ray diffraction structure of the resting state of component 1 (EPM) shows the cofactor to be about 10 Å below the surface of the protein without an obvious path for substrate or inhibitor entrance (*2, 3, 5*). The open form of the E* structure may provide such a path (*39*) and explains why the rates of both substrate reduction (relative to H_2 evolution) and hi-CO formation are similar during low electron flux.

There are several problems with both the redox and structural state hypotheses for the formation of the hi-CO structure. Like EPM, state $[EPM]^{2-}$ is an odd electron state (as are $EP[M(CO)_2]$ and $EP[M(CO)_2]^{2-}$) and should be observable by EPR spectroscopy. Except for the inflections observed at high flux under CO (Figure 2, as discussed

below), no new signals have been observed by us during steady-state turnover. Since all of the iron in EP[M^-] is ferrous (*9*), state [EPM]$^{2-}$ exists through either the reduction of Mo^{4+} to Mo^{3+} or the reduction of a nonmetal site in the protein. During turnover, no nonmetal free radical EPR signals have been detected. A similar problem exists with the structural state hypothesis; i.e., since no new structural state E* has been detected, there are no experimental data to support its existence. Therefore, at present there is no way of favoring one hypothesis over the other.

Whether due to a redox or structural state, the rate of formation of either hi-CO or lo-CO should be about the same. The ability to detect hi-CO but not lo-CO during very low electron flux thus suggests that the lo-CO structure has a greater rate of decay [rate (3) ≥ rate (2)]. This interpretation is in agreement with our study of the decay of hi-CO and lo-CO during turnover which also showed rate (3) ≥ rate (2). As the electron flux increases, the rate of formation of lo-CO becomes greater than the rate of decay, and lo-CO becomes detectable.

The dependency of the steady-state concentration of hi-CO on the [Av2]/[Av1] component ratio is similar to that of M in the absence of CO. Specifically, as the component ratio increases from 1:100 to 1:5, the steady-state concentration of either M or hi-CO decreases. An additional increase in the component ratio to 1:1 in the presence of CO (and 5× normal [ATP]) produces two new signals ($g = 5.78$, 5.15 and $g = 1.95$, 1.81) (Figure 2B).

Origin of the New EPR Signals. Several different signals in the $g = 5$ region have been observed previously with nitrogenase. Inflections at $g = 5.7$ and 5.4 were detected in nitrogenase samples of *Klebsiella pneumoniae* during turnover under Ar (*14*) and assigned to a state with $S > 3/2$. Similar signals at $g = 5.7$ and 5.4, albeit of extremely low intensities, have been observed with *K. pneumoniae* nitrogenase during turnover (*40*) in the presence of N_2 (but were absent when CO was present) and were suggested to arise from oxidized P clusters [P^{3+} was previously detected at $g = 5.5$ for Av1 (*41*)]. Single oxidation of P clusters (P → P^+) in Av1 also generates a signal at $g = 5.30$ assigned (Table 1) to an excited-state ($g_{\pm 1/2}$) inflection of an $S = 5/2$ spin system (*33*). Finally, nitrogenase component 2 also exhibits broad inflections at $g = 5.88$ and 4.70 assigned to an $S = 3/2$ mixed-spin state of the $[4Fe\text{-}4S]^+$ cluster (*42, 43*).

The inflections at $g = 5.78$ and 5.15 in the presence of CO (Figure 2B) are significantly different from all of the above signals and represent a previously unobserved state of the enzyme. Temperature-dependent studies (data not shown) show that these inflections are associated with an $S = 3/2$ spin system ($D = 0.43$ cm^{-1} and $E/D = 0.22$) with predicted g-factors (using $g_e = 2.016$) of $g_x = 2.64$, $g_y = 5.15$, and $g_z = 1.75$ for the ground (pseudo $m_s = \pm 1/2$) state and $g_x = 1.39$, $g_y = 1.12$, and $g_z = 5.78$ for the first-excited (pseudo $m_s = \pm 3/2$) state. This assignment is strengthened by the observation of a weak broad inflection at $g = 2.7$ (Figure 2B) assigned to g_x in the ground state.

The origin of the second signal at $g = 1.95$, 1.81 is easily identified. These inflections have been observed previously (*33*) during oxidative titration of Av1 and arise from an $S = 1/2$ state of the singly oxidized P clusters (P → P^+). Oxidation of P cluster has been suggested as a mechanistic step in the reduction of dinitrogen (*5*). Absorbancy increases at 430 nm have been detected in stopped-flow experiments and assigned to P cluster oxidation while EPR inflections at $g = 5.7$ and 5.4 have been observed in turnover samples and suggested to arise from oxidized P cluster (*40*), possibly P^{3+}. These latter signals, however, were not observed when CO was present. The fact that the $g = 1.95$, 1.81 signal observed is nearly identical in shape, spectral position, and temperature dependency to signals associated with P^+ (*33*) definitively shows that P cluster oxidation (P → P^+) occurs during catalysis in the presence of CO (Figure 2).

Chemical oxidation of P → P^+ in Av1 generates not only the $g = 1.95$, 1.81 signal described above but also an $S = 5/2$ signal at $g = 6.67$ and 5.30 (*33*). The P cluster is composed of two [4Fe-3S] cuboidal structures bridged by a single sulfide (*6*). If we symbolize each [4Fe-3S] structure by C, then the P cluster can be written as C_α-S-C_β since one structure (C_α) is predominantly bound to the α polypeptide while the other structure (C_β) is mainly bound to the β polypeptide. It has been suggested (*33, 44, 45*) that the two P^+ signals ($S = 5/2$ and $S = 1/2$) represent single oxidation of separate [4Fe-3S] structures of the P cluster. Specifically, the suggestion is that both halves possess approximately the same midpoint potential (*44, 46*) such that single oxidation (P → P^+) randomly generates both $C_\alpha{}^+$-S-C_β and C_α-S-$C_\beta{}^+$ rather than a delocalized paramagnetism over the entire cluster, $[C_\alpha\text{-S-}C_\beta]^+$. This interpretation is strengthened by the finding that single oxidation of the P cluster in the VFe protein from *A. vinelandii* generates only the $S = 5/2$ signal (*45*). This suggests that the two halves of C_α-S-C_β in the VFe protein possess different midpoint potentials such that the $S = 5/2$ side of the P cluster is initially oxidized in preference to the other side. It is interesting that while chemical oxidation of the P clusters of Av1 generates both $S = 5/2$ and $S = 1/2$ signals, turnover oxidation generates only the $S = 1/2$ signal.

Since the $g = 1.95$, 1.81 signal in Figure 2B arises from P^+ and the $g = 5.78$, 5.15 signal is not associated with any known oxidation state of either the P cluster or the Fe protein, this latter signal may be associated with the CO-bound cofactor. One possibility is that it is the TL doubly reduced state of the enzyme with CO bound, $[EPM(CO)_2]^{2-}$. Another possibility is that it arises from the CO-bound cofactor in the activated structure of the enzyme (E*P[$M(CO)_2$]) with a spin ($S = 3/2$) different from the resting state structure of hi-CO (EP[$M(CO)_2$] with $S = 1/2$, Table 1). Both $[EPM(CO)_2]^{2-}$ and E*P[$M(CO)_2$] are odd electron states and would yield half-integer spin signals.

The oxidation of the P cluster to yield the $g = 1.95$, 1.81 signal probably occurs through an *intramolecular* electron transfer from the P cluster to the cofactor. Intramolecular electron transfer from P to M previously has been suggested (*39*) and has been detected during oxidative titration of a unique structural $\alpha\beta_2$ form of the VFe protein of V-nitrogenase (*19, 45*). Intramolecular electron transfer also provides a explanation of why only the $g = 1.95$, 1.81 ($S = 1/2$) P^+ signal is observed during turnover and not the $g = 6.67$, 5.30 ($S = 5/2$) P^+ signal. The X-ray diffraction structure of Av1 shows (*6, 47*) that one side of the P cluster (the side bound mainly to the α subunit, or C_α) is closer to the cofactor than the other side (β-bound or C_β). While chemical oxidation (P → P^+) would randomly generate both

C_α^+-S-C_β and C_α-S-C_β^+, intramolecular electron transfer (eq 12) should favor the oxidation of the side closer to the cofactor ($C_\alpha \rightarrow C_\alpha^+$). Assuming that intracluster electron transfer (C_α^+-S-$C_\beta \leftrightarrow C_\alpha$-S-$C_\beta^+$) is very slow or nonexistent, this interpretation allows the structural assignment of the two spin states of P^+; i.e., $S = 1/2$ is associated with C_α^+-S-C_β while $S = 5/2$ arises from C_α-S-C_β^+.

Results from ethylene glycol (EG) quenching experiments (Figure 5) give us additional information about the lo-CO and hi-CO structures. First, EG inhibits the decay of hi-CO in the *absence* of turnover as long as CO is present in the environment. Second, EG stabilizes the lo-CO structure, making it resistant to decay even in the absence of CO in the gas phase. Third, the interconversion between lo-CO and hi-CO requires neither turnover nor electron transfer. Turnover is only needed to generate the state (redox or structural) necessary for the formation of the lo-CO and hi-CO structure. Once these structures are formed, EG stabilizes them and allows CO to be easily added to or taken off of the cofactor (i.e., hi-CO $\leftrightarrow$ lo-CO + CO).

Conclusions. (1) Formation of lo-CO or hi-CO requires a redox or structural state, generated only during turnover, that is different from EPM or EP[M^-]. (2) During turnover, CO dissociates from the cofactor in about 10 min. (2) Rapid EG quenching of turnover stabilizes lo-CO. (3) Interconversion between lo-CO and hi-CO does not require turnover. (4) P cluster oxidation is observed during turnover in the presence of CO at high component ratios and elevated [ATP].

ACKNOWLEDGMENT

We thank the Pennington Biomedical research facility for use of their EPR spectrometer.

REFERENCES

1. Georgiadis, M. M., Komiya, H., Chakrabarti, P., Woo, D., Kornuc, J. J., and Rees, D. C. (1992) *Science 257*, 1653−1659.
2. Kim, J., and Rees, D. C. (1992) *Science 257*, 1677−1682.
3. Kim, J., and Rees, D. C. (1992) *Nature 360*(10), 553−560.
4. Bolin, J. T., Campobasso, N., Muchmore, S. W., Morgan, T. V., and Mortenso, L. E. (1993) in *Molybdenum Enzymes, Cofactors, and Model Systems* (Stiefel, E. I., Coucouvanis, D., and Newton, W. E., Eds.) pp 186−195, American Chemical Society, Washington, D.C.
5. Chan, M. K., Kim, J., and Rees, D. C. (1993) *Science 260*, 792−794.
6. Peters, J. W., Stowell, M. H. B., Soltis, S. M., Finnegan, M. G., Johnson, M. K., and Rees, D. C. (1997) *Biochemistry 36*(6), 1181−1187.
7. Pollock, R. C., Lee, H.-I., Cameron, L. M., DeRose, V. J., Hales, B. J., Orme-Johnson, W. H., and Hoffman, B. M. (1995) *J. Am. Chem. Soc. 117*, 8686−8687.
8. Christie, P. D., Lee, H.-I., Cameron, L. M., Hales, B. J., Orme-Johnson, W. H., and Hoffman, B. M. (1996) *J. Am. Chem. Soc. 118*, 8707−8709.
9. Lee, H.-I., Hales, B. J., and Hoffman, B. M. (1997) *J. Am. Chem. Soc. 119*, 11395−11400.
10. Lee, H.-I., Cameron, L. M., Hales, B. J., and Hoffman, B. M. (1997) *J. Am. Chem. Soc. 119*, 10121−10126.
11. Hwang, J. L., Chen, C. H., and Burris, R. H. (1973) *Biochim. Biophys. Acta 292*, 256−270.
12. Burgess, B. K. (1985) in *Molybdenum Enzymes* (Spiro, T. G., Ed.) pp 161−220, John Wiley and Sons, New York.
13. Yates, M. G., and Lowe, D. J. (1976) *FEBS Lett. 72*(1), 121−126.
14. Lowe, D. J., Eady, R. R., and Thorneley, R. N. F. (1978) *Biochem. J. 173*, 277−290.
15. Orme-Johnson, W. H., and Davis, L. C. (1978) in *Iron−Sulfur Proteins* (Lovenberg, W., Ed.) pp 15−60, Academic, New York.
16. Davis, L. C., Henzl, M. T., Burris, R. H., and Orme-Johnson, W. H. (1979) *Biochemistry 18*(22), 4860−4869.
17. George, S. J., Ashby, G. A., Wharton, C. W., and Thorneley, R. N. F. (1997) *J. Am. Chem. Soc. 119*, 6450−6451.
18. Burgess, B. K., Jacobs, D. B., and Stiefel, E. I. (1980) *Biochim. Biophys. Acta 614*, 196−209.
19. Blanchard, C. Z., and Hales, B. J. (1996) *Biochemistry 35*, 472−478.
20. Hagen, W. R. (1992) in *Advances in Inorganic Chemistry: Iron−Sulfur Proteins* (Sykes, A. G., and Cammack, R., Eds.) pp 165−222, Academic Press, New York.
21. Hageman, R. V., and Burris, R. H. (1978) *Proc. Natl. Acad. Sci. U.S.A.* 75(6), 2699−2702.
22. Fischer, K., Lowe, D. J., and Thornley, R. N. F. (1991) *Biochem. J. 279*, 81−85.
23. Münck, E., Rhodes, H., Orme-Johnson, W. H., Davis, L. C., Brill, W. J., and Shah, V. K. (1975) *Biochim. Biophys. Acta 400*, 32−53.
24. Hageman, R. V., and Burris, R. H. (1978) *Proc. Natl. Acad. Sci. U.S.A. 75*(6), 2699−2702.
25. Thorneley, R. N. F., and Lowe, D. J. (1985) in *Molybdenum Enzymes* (Spiro, T. G., Ed.) pp 221−284, John Wiley and Sons, New York.
26. Orme-Johnson, W. H., Hamilton, W. D., Ljones, T., Tso, M.-Y. W., Burris, R. H., Shah, V. K., and Brill, W. J. (1972) *Proc. Natl. Acad. Sci. U.S.A. 69*, 3142−3145.
27. Smith, B. E., Lowe, D. J., and Bray, R. C. (1972) *Biochem. J. 130*, 641−643.
28. Smith, B. E., Lowe, D. J., and Bray, R. C. (1973) *Biochem. J. 135*, 331−341.
29. Zumft, W. G., Mortenson, L. E., and Palmer, G. (1974) *Eur. J. Biochem. 46*, 525−535.
30. Zimmermann, R., Münck, E., Brill, W. J., Shah, V. K., Henzl, M. T., Rawlings, J., and Orme-Johnson, W. H. (1978) *Biochim. Biophys. Acta 536*, 185−207.
31. Rawlings, J., Shah, V. K., Chisnell, J. R., Brill, W. J., Zimmermann, R., Münck, E., and Orme-Johnson, W. H. (1978) *J. Biol. Chem. 253*(4), 1001−1004.
32. Huynh, B. H., Münck, E., and Orme-Johnson, W. H. (1979) *Biochim. Biophys. Acta 527*, 192−203.
33. Tittsworth, R. C., and Hales, B. J. (1993) *J. Am. Chem. Soc. 115*(21), 9763−9767.
34. Schultz, F. A., Gheller, S. F., Burgess, B. K., Lough, S., and Newton, W. E. (1985) *J. Am. Chem. Soc. 107*(19), 5364−5368.
35. Lowe, D. J., and Thorneley, R. N. F. (1984) *Biochem. J. 224*, 877−886.
36. Lowe, D. J., and Thorneley, R. N. F. (1984) *Biochem. J. 224*, 895−901.
37. Thorneley, R. N. F., and Lowe, D. J. (1984) *Biochem. J. 224*, 887−894.
38. Thorneley, R. N. F., and Lowe, D. J. (1984) *Biochem. J. 224*, 903−909.
39. Howard, J., and Rees, D. (1994) *Annu. Rev. Biochem. 63*, 235.
40. Lowe, D. J., Fisher, K., and Thorneley, R. N. F. (1993) *Biochem. J. 292*, 93−98.
41. Hagen, W. R., Wassink, H., Eady, R. R., Smith, B. E., and Haaker, H. (1987) *Eur. J. Biochem. 169*, 457−465.
42. Lindahl, P. A., Day, E. P., Kent, T. A., Orme-Johnson, W. H., and Münck, E. (1985) *J. Biol. Chem. 260*, 11160−11173.
43. Onate, Y. A., Finnegan, M. G., Hales, B. J., and Johnson, M. K. (1993) *Biochim. Biophys. Acta 1164*, 113−123.
44. Oliver, M. E., and Hales, B. J. (1992) *J. Am. Chem. Soc. 114*, 10618−10623.
45. Tittsworth, R. C., and Hales, B. J. (1996) *Biochemistry 35*, 479−489.
46. Pierik, A. J., Wassink, H., Haaker, H., and Hagen, W. R. (1993) *Eur. J. Biochem. 212*, 51−61.
47. Kim, J., and Rees, D. C. (1992) *Science 257*, 1677−1682.

BI972667C